Continuous attractor network models of grid cell firing based on excitatory-inhibitory interactions

1 **Continuous attractor network models of grid cell firing based on**
2 **excitatory-inhibitory interactions**
3
4 Oliver Shipston-Sharman [1], Lukas Solanka [1], Matthew F. Nolan [1]
5
6 [1] Centre for Integrative Physiology, University of Edinburgh, Hugh Robson
7 Building, Edinburgh, EH8 9XD, United Kingdom
8
9
10 *Corresponding author:*
11 Matthew F. Nolan
12 Centre for Integrative Physiology, University of Edinburgh, Hugh Robson
13 Building, Edinburgh, EH8 9XD, United Kingdom
14 +44 131 650 9874
15 mattnolan@ed.ac.uk
16
17 *Keywords:* Gamma oscillation, recurrent network, neural computation,
18 excitation, inhibition, epilepsy
19
20
21 **Key points summary:**
22
23 1. Neurons with grid firing fields are thought to encode estimates of location
24 computed from self-motion signals.
25
26 2. Evidence points towards continuous attractor networks as a substrate for
27 grid firing, but the cellular mechanisms are not well understood.
28
29 3. Computational models of excitatory and inhibitory cells with realistic
30 membrane dynamics account for grid firing and related network oscillations.
31
32 4. We argue that investigation of predictions from models of this kind will be
33 essential to establish mechanisms for grid firing and other cognitive
34 computations.
35
36

Abstract

Neurons in the medial entorhinal cortex encode location through spatial firing fields that have a grid-like organisation. The challenge of identifying mechanisms for grid firing has been addressed through experimental and theoretical investigations of medial entorhinal circuits. Here, we discuss evidence for continuous attractor network models that account for grid firing by synaptic interactions between excitatory and inhibitory cells. These models assume that grid-like firing patterns are the result of computation of location from velocity inputs, with additional spatial input required to oppose drift in the attractor state. We focus on properties of continuous attractor networks that are revealed by explicitly considering excitatory and inhibitory neurons, their connectivity and their membrane potential dynamics. Models at this level of detail can account for theta-nested gamma oscillations as well as grid firing, predict spatial firing of interneurons as well as excitatory cells, show how gamma oscillations can be modulated independently from spatial computations, reveal critical roles for neuronal noise, and demonstrate that only a subset of excitatory cells in a network need have grid-like firing fields. Evaluating experimental data against predictions from detailed network models will be important for establishing the mechanisms mediating grid firing.

Abbreviations: MEC, medial entorhinal cortex; L2SCs, layer 2 stellate cells; L2PCs, layer 2 pyramidal cells; E-I, excitatory-inhibitory; PV, parvalbumin.

Introduction

Neural representations of space within the hippocampus and medial entorhinal cortex (MEC) are critical for navigation and memory. Grid cells in the MEC have firing fields that encode position using an allocentric, regular triangular matrix or *grid*-like firing pattern (Hafting et al., 2005). Grid representations have the properties of a high capacity, high resolution and error correcting code for self-localisation (Fiete et al., 2008; Mathis et al., 2012; Sreenivasan and Fiete, 2011). The spatially periodic features of grid firing fields have led to the view that they are the output of computation by a path integrator that translates self-motion signals into estimates of location (McNaughton et al., 2006). In this review, we will consider evidence that network attractor dynamics arising from excitatory-inhibitory interactions account for grid firing patterns within MEC circuits.

The organisation within the MEC of spatial firing properties is an important constraint on mechanistic models for grid firing. Grid cells form networks in anatomically overlapping but functionally discrete modules, with cells of the same module sharing their grid spacing and orientation but having randomly distributed phases (relative offset of grid apices) (Barry et al., 2007; Hafting et al., 2005; Stensola et al., 2012). The highest density of grid cells is in layer 2 of the MEC (Sargolini et al., 2006). Grid cells in this layer also show the greatest prospective bias in their code for location (Kropff et al., 2015). There are two major populations of excitatory cells in this layer. Neurons positive for the marker reelin have stellate morphology and project to the dentate gyrus of the hippocampus (Klink and Alonso, 1997; Varga et al., 2010), while neurons positive for calbindin have a more pyramidal morphology and project to the CA1 region of the hippocampus (Kitamura et al., 2014; Ray et al., 2014; Varga et al., 2010). We will refer to these cell populations as layer 2 stellate cells (L2SCs) and layer 2 pyramidal cells (L2PCs) respectively (Klink and Alonso, 1997)(L2SCs and L2PCs have also been referred to as 'Ocean' and 'Island' cells (Kitamura et al., 2014)). Both L2SCs and L2PCs may have grid firing fields, although the majority of neurons in each population do not appear to generate typical grid firing patterns (Sun et al., 2015; Tang et al., 2014). During behaviours that produce grid firing, neurons in superficial layers of the

3

95 MEC also generate fast gamma frequency (60-140 Hz) oscillations that are
96 modulated by the slower theta rhythm (Chrobak and Buzsaki, 1998; Colgin et
97 al., 2009). While all grid cells encode location through their firing rate, some
98 also represent location through timing of their action potentials relative to the
99 network theta rhythm (Hafting et al., 2008; Reifenstein et al., 2012).

101 Several conceptual models have been proposed to explain grid firing patterns
102 (for reviews see (Burgess and O'Keefe, 2011; Giocomo et al., 2011; Zilli,
103 2012)). However, implementing models in ways that are consistent with the
104 biophysics and connectivity of entorhinal neurons is challenging (Pastoll et al.,
105 2012; Remme et al., 2010). Here, we will explore insights from models in
106 which grid-like firing patterns emerge as a result of path integration in
107 continuous attractor networks composed of excitatory and inhibitory neurons,
108 with membrane potential dynamics that approximate real neurons (Figure 1).
109 We will argue that this class of models is particularly useful as they can be
110 constrained by experimentally measured synaptic connectivity and oscillatory
111 network activity, as well as by action potential firing during spatial behaviours.
112 They therefore generate specific predictions that are testable by diverse
113 experimental approaches from anatomical analysis through to
114 electrophysiological recordings of single cell and network activity.

116 **Continuous attractors networks as models for grid generation**

117 Continuous attractor networks are dynamical systems whose intrinsic
118 properties drive activity towards a stable state; this can be visualised in a
119 state space comprising an energy surface upon which stable states are
120 represented by low energy regions (Brody et al., 2003). States existing
121 outwith these regions will decay 'downwards' towards the low energy points. A
122 network's intrinsic connections can be configured so its preferred states will
123 correspond to localised bumps of activity. Mathematical functions can then be
124 implemented in the network's state space by movement of the bumps of
125 activity in response to inputs to the network (Conklin and Eliasmith, 2005;
126 Eliasmith, 2005). In continuous attractor network models of spatial coding, the

4

127   computation performed is integration of velocity input to generate an estimate

128   of location relative to a known start point, referred to as path integration

129   (McNaughton et al., 1996; McNaughton et al., 2006; Samsonovich and

130   McNaughton, 1997; Zhang, 1996). Such networks do not necessarily

131   generate triangular grid-like firing fields, but can do so with appropriately

132   configured connections. In networks that model grid firing, stable states

133   manifest either as a bump (Figure 2A) or as multiple bumps of activity (Figure

134   2B) on a two-dimensional sheet of phase-arranged grid cells (Fuhs and

135   Touretzky, 2006; Guanella et al., 2007). Given velocity inputs the activity

136   bump(s) represent movement in space by propagating across the sheet. This

137   mechanism for path integration can be implemented by networks in which

138   individual grid cells receive velocity inputs tuned to a particular movement

139   direction, with the local connections of each grid cell offset so that an increase

140   in its input will tend to push the activity bump in an appropriate direction

141   across the neural sheet (Burak and Fiete, 2009; Fuhs and Touretzky, 2006;

142   Guanella et al., 2007). Alternatively, path integration could be achieved

143   through interactions between a layer of heading-independent grid cells and

144   multiple layers of head direction-modulated grid cells, which each integrate a

145   single head direction input with speed signals and feedback from the heading-

146   independent grid layer (Samsonovich and McNaughton, 1997). While the

147   latter class of models require many more neurons to account for path

148   integration, because separate layers are required for each heading direction,

149   they have the advantage that they naturally account for direction modulated

150   (or conjunctive) grid cells as well as pure grid cells.

151

152   Continuous attractor network models have been implemented at various

153   levels of detail and a close correspondence to known neural connectivity or

154   dynamics is not necessary to generate grid-like firing fields. Indeed,

155   experimental observations have corroborated a number of generic predictions

156   that are independent of the details of the circuitry used for model

157   implementation (McNaughton et al., 2006). 1. Populations of grid cells are

158   organised into modules in which each neuron has a common spatial phase

159   and orientation (Stensola et al., 2012). 2. The spatial phase relationship

160   between cells is maintained even following environmental manipulations that

161 restructure the spatial firing pattern of individual cells (Yoon et al., 2013). 3.
162 The envelope of the membrane potential of grid cells changes slowly on entry
163 to and exit from their firing fields (Domnisoru et al., 2013; Schmidt-Hieber and
164 Hausser, 2013). 4. Removal of excitatory drive causes cells that previously
165 had grid fields to encode head direction (Bonnevie et al., 2013), which is
166 consistent with movement of activity bumps in continuous attractor networks
167 relying on each grid cell receiving a tuned head direction input (Bonnevie et
168 al., 2013; Burak and Fiete, 2009; Fuhs and Touretzky, 2006; Guanella et al.,
169 2007; Pastoll et al., 2013).

171 While these observations are consistent with continuous attractor network
172 models accounting for rate coded grid fields, most existing models do not
173 readily account for precession in the timing of action potentials fired by some
174 grid cells relative to the theta rhythm (Hafting et al., 2008; Reifenstein et al.,
175 2012). One-dimensional attractor networks, based on interaction between a
176 direction-independent cell population and direction modulated cell
177 populations, can generate repeating firing fields and phase precession
178 (Navratilova et al., 2012). Extension of this mechanism to two dimensions will
179 require additional neuronal layers for each heading direction (Samsonovich
180 and McNaughton, 1997). An alternative is that phase precession and attractor
181 states are established independently. For example, phase precession can be
182 explained by hybrid models that include a mechanism for grid firing based on
183 interference between oscillations (Burgess et al., 2007; Hasselmo et al.,
184 2007), in addition to mechanisms for generation of network attractor states
185 (Bush and Burgess, 2014; Schmidt-Hieber and Hausser, 2013).

187 **Emergence of attractor states through excitatory-inhibitory interactions**
188 How might attractor mechanisms for grid firing be implemented in networks of
189 neurons? Do the properties of neural circuitry in the MEC constrain models or
190 lead to predictions that distinguish between different models? Grid
191 computation in continuous attractor networks requires emergence of stable
192 bumps of activity. This can be achieved using reduced models in which
193 separate populations of excitatory and inhibitory neurons are not explicitly
194 considered. In these models, either each neuron locally excites nearby

6

195   neurons and inhibits more distant neurons (Fuhs and Touretzky, 2006), or

196   spatially structured inhibitory connections act in concert with excitatory drive

197   to the whole network (Burak and Fiete, 2009; Couey et al., 2013). However,

198   use of local excitatory connections is inconsistent with evidence that L2SCs

199   are not directly connected to one another (Dhillon and Jones, 2000; Pastoll et

200   al., 2013; Couey et al., 2013), but instead interact indirectly via inhibitory

201   interneurons (Pastoll et al., 2013; Couey et al., 2013). Moreover, because grid

202   cells are excitatory neurons, an inhibitory output from grid cells is inevitably an

203   over-simplification. One could address this by assuming that the inhibitory

204   output from grid cells is equivalent to an excitatory connection to a dedicated

205   inhibitory interneuron. However, this is inconsistent with convergent (many to

206   one) and divergent (one to many) connectivity between excitatory and

207   inhibitory networks (Couey et al., 2013), and with there being many more

208   excitatory than inhibitory neurons in layer 2 of the MEC (Canto et al. 2008).

209   Thus, while offering conceptually important explanations for grid firing,

210   reduced models are limited in their ability to evaluate consequences of

211   experimentally determined connectivity.

212

213   Models that explicitly consider interactions between separate populations of

214   excitatory and inhibitory neurons inevitably differ from reduced models,

215   leading to new insights and predictions (Pastoll et al., 2013; Solanka et al.,

216   2015; Widloski and Fiete, 2014). Given appropriately structured network

217   connectivity these excitatory-inhibitory (E-I) models generate network attractor

218   states (Figure 2). Structured connectivity can be implemented by varying the

219   strength of connections between neurons according to their position in the

220   network, while maintaining a fixed probability of a connection being present

221   (Pastoll et al., 2013; Solanka et al., 2015; Widloski and Fiete, 2014).

222   Alternatively, synaptic strength can remain fixed but the probability of

223   connections varied as a function of distance between pre- and postsynaptic

224   neurons on the neural sheet (Solanka et al., 2015). Evidence that the

225   amplitude of inhibitory inputs to stellate cells has a bimodal distribution is

226   consistent with structuring of connection probability rather than the strength of

227   connections (Couey et al 2013). Models based on E-I interactions also

228   demonstrate that velocity inputs, which are required for movement-dependent

229   translation of their activity bumps, may target either interneurons or excitatory
230   cells (Pastoll et al. 2013). While spatial firing of cells with inhibitory output is
231   implicit in reduced models, in E-I models interneurons have spatial firing fields
232   that depend on the wiring of the network. For example, either surround
233   inhibition or surround excitation supports grid firing by excitatory cells, but in
234   the latter case interneurons have inverted grid fields, whereas in the former
235   they have grid-like fields (Pastoll et al. 2013).

236

237   Two important recent experimental studies introduce challenges beyond
238   simply accounting for grid firing by excitatory cells. First, while the firing fields
239   of parvalbumin (PV) positive interneurons have significant spatial stability,
240   they typically have grid scores below the threshold for grid firing, only rarely
241   appear to have a clear grid like organisation (Buetfering et al. 2014), and on
242   visual inspection also do not appear to have inverted firing fields although this
243   is difficult to establish quantitatively. Second, when layer 2 cells are imaged in
244   freely moving animals, only about 10 % of identified L2SCs and L2PCs have
245   grid-like firing fields (Sun et al., 2015). This is surprising given that neurons
246   within each population appear to have similar synaptic connectivity and
247   intrinsic properties. This could suggest that the grid firing neurons correspond
248   to sub-groups of cells with distinct, but not yet identified, cellular or circuit
249   properties. Otherwise, models for grid firing must explain how grid patterns
250   are produced by only a subset of neurons that at a cellular and circuit level
251   are indistinguishable from non-grid cells.

252

253   These challenges may be addressed using E-I networks and by considering
254   that in vivo entorhinal neurons may receive spatial signals that can be
255   considered as noise in the sense that they are not used to promote grid firing.
256   Thus, when E-I models are extended to include random spatial input to
257   interneurons, excitatory neurons in these networks continue to generate grid-
258   like firing fields, but the hexagonal symmetry of interneuron firing fields is
259   reduced (Figure 3)(Solanka et al. 2015). In these networks the fraction of
260   excitatory and inhibitory cells classified as grid cells drops substantially, with
261   almost no interneurons classified as having grid fields (Figure 3). Thus, the
262   finding that only a subset of layer 2 cells have grid-like firing fields need not

263   imply that grid and non-grid cells are distinguished by distinct cellular or circuit

264   properties, while the absence of a clear grid signature in the firing of individual

265   interneurons may nevertheless be compatible with models based on E-I

266   interactions.

267

268   **Single and multi-bump networks differ in their local and long-range**

269   **connectivity**

270   Continuous attractor network models for grid firing exist in versions that differ

271   in their number of activity bumps. These functional differences result primarily

272   from connections spanning different distances relative to the size of the

273   network.

274

275   In single bump networks (also referred to as periodic networks, cf. Widlowski

276   and Fiete, 2015) the planar attractor manifold is wrapped into a torus

277   (Guanella et al., 2007; Pastoll et al., 2013; Samsonovich and McNaughton,

278   1997). This conceptual torus structure is actuated in the synaptic connectivity

279   of the network, with cells on one edge of the sheet connected to those on the

280   opposite side (Figure 2A). When an animal travels continuously in one

281   direction the activity bump moves periodically around the network. Generation

282   of a triangular rather than rectangular organisation of grid fields is dependant

283   on the addition of a phase shift in one axis resulting in a twisted torus attractor

284   manifold (Figure 2A).

285

286   Networks with multiple bumps of activity also have their neurons arranged on

287   a two dimensional manifold, however, a hexagonal population activity bump

288   organisation arises from the most energetically efficient packing of the rings of

289   inhibition; each circle of inhibition repels neighbouring circles to a maximal

290   distance until stabilising into a grid of activity bumps (Figure 2B)(Burak and

291   Fiete, 2009; Couey et al., 2013; Fuhs and Touretzky, 2006). During

292   movement the bumps of activity propagate across the network and individual

293   neurons generate grid firing patterns. Multi-bump networks can either be

294   implemented with periodic boundaries (also referred to as partially periodic

295   networks), so that much as in single bump models the activity bump wraps to

296   the other side of the network. Alternatively, they can have boundaries (also

9

297 referred to as aperiodic networks). In this case, when bumps reach the edge
298 of the network they disappear, while on the opposite side of the network local
299 competitive synaptic interactions cause new bumps to spontaneously form as
300 existing bumps move away (Burak and Fiete, 2009; Fuhs and Touretzky,
301 2006).

302

303 When single bump attractors are implemented in E-I networks, each neuron's
304 connections extend over a relatively large fraction of the network (Figure 2A).
305 Thus, neurons making surround connections have their highest connection
306 probability, or connection strength, with neurons at a distance of
307 approximately half the width of the untwisted neural sheet. This distance
308 refers to separation based on the order of connectivity in the network rather
309 than anatomical distance (cf. (Widloski and Fiete, 2014)). Indeed the
310 anatomical organisation of cell bodies of neurons with repeating firing fields
311 appears relatively weak compared to the organisation of neural sheets in
312 continuous attractor network models (Heys et al., 2014), suggesting that
313 synaptic connectivity required for grid firing can be established without
314 ordering of neuronal cell bodies (Widloski and Fiete, 2014). In contrast to
315 single bump networks, the connectivity in multi-bump attractors is much more
316 localised relative to the overall size of the network (Figure 2B). This suggests
317 that quantification of the extent of connectivity between excitatory and
318 inhibitory neurons could be used to distinguish between single and multi-
319 bump models. Local circuit perturbations through thermo- or chemo-
320 modulation in conjunction with multi-unit recordings might also distinguish
321 between single and multi-bump networks (Widloski and Fiete, 2015).

322

323 **Excitatory-inhibitory interactions provide a common mechanism for grid**
324 **firing and network oscillations**
325 Successful models of brain circuits should account for network dynamics as
326 well as the firing patterns of individual cells. Dynamics can be modelled by
327 simulating networks of integrate and fire neurons. In these models synaptic
328 input to a neuron charges its membrane capacitance, which is in turn
329 discharged through a resistance. Action potentials occur when the membrane
330 potential crosses a threshold. In exponential integrate and fire neurons the

331   spike threshold has been replaced with an exponential function in order to
332   obtain more realistic spike initiation dynamics (Fourcaud-Trocme et al., 2003).
333   Although integrate and fire models neglect details of morphology and ion
334   channel biophysics, their dynamics are a good approximation for physiological
335   synaptic integration, making them an important bridge between abstract
336   theoretical and more detailed cellular models.

337

338   Models of interacting populations of excitatory and inhibitory exponential
339   integrate and fire neurons can account for both grid firing and gamma
340   oscillations (Pastoll et al. 2013, Solanka et al. 2015). When the models
341   receive theta modulated input the gamma oscillations are nested at a fixed
342   phase within each theta cycle (Figure 4). This is consistent with experimental
343   findings that theta modulated optogenetic activation of layer 2 circuits is
344   sufficient to generate nested gamma activity resembling that observed in
345   behaving animals (Pastoll et al. 2013, Chrobak et al. 2000). In these
346   experiments, and in the corresponding models, gamma oscillations emerge
347   through fast time scale E-I interactions. On each gamma cycle a subset of
348   excitatory neurons fire action potentials. Because the output from each
349   excitatory neurons diverges to many interneurons (Figure 2A), and as each
350   interneuron receives convergent input from many excitatory cells (Figure 2A),
351   this output is sufficient to rapidly trigger action potentials in a large fraction of
352   interneurons. Divergent projections from interneurons send inhibitory
353   feedback to excitatory cells, including those that did not spike. A second
354   gamma cycle is initiated on recovery from this inhibition. The divergent
355   connectivity effectively implements a competitive mechanism that limits the
356   number of excitatory cells active on each theta cycle (Tiesinga and Sejnowski,
357   2009). While E-I models account for both rate coded firing and nested gamma
358   oscillations, a possible limitation of existing models is that theta input is
359   implemented as a common drive to E and I cells. In contrast, only
360   interneurons in the MEC appear to receive inhibitory pacemaker input from
361   the medial septum (Gonzalez-Sulser et al., 2014) while the origin of excitation
362   during theta is currently unknown.

363

364 Models that account for grid firing and nested gamma oscillations exclusively

365 through E-I interactions have been extended to incorporate additional features

366 of MEC circuitry (Solanka et al. 2015). Experimental observations indicate that

367 inhibitory neurons in layer 2 of the MEC may synapse with one another

368 (Pastoll et al. 2013). Addition to E-I models of connections between

369 interneurons stabilises grid firing and increases the frequency of nested

370 gamma oscillations (Solanka et al. 2015). The resulting E-I-I models more

371 easily produce theta oscillations with frequency that matches that of gamma

372 activity in vivo (cf. Chrobak et al. 1998, Colgin et al. 2012). Although E-I

373 models were initially motivated by the indirect connectivity between L2SCs,

374 grid cells are found in deeper layers in which excitatory cells are likely to

375 communicate directly with one another (Dhillon and Jones, 2000). Moreover,

376 while many models for grid firing have focussed on L2SCs, L2PCs also have

377 grid firing fields (Sun et al., 2015), and the synaptic mechanisms through

378 which they interact may differ. When E-I models are extended to include

379 structured connectivity between excitatory neurons in addition to structured E-

380 I interactions they continue to generate grid firing patterns (Widloski and Fiete,

381 2014) and nested gamma oscillations (Solanka et al. 2015). However, when

382 these models were modified further so that inhibitory connectivity is random

383 and only excitatory connectivity is structured they were unable to generate

384 stable grid firing fields (Solanka et al. 2015). We suspect this results from

385 requirements for precise tuning of connections in continuous attractor

386 networks based on structured excitation (cf. (Seung et al., 2000)).

387

388 The strong theta frequency modulation of activity in the MEC raises the

389 question of how attractor states might be maintained during phases of the

390 theta cycle in which activity is suppressed. In principle if activity is suppressed

391 for a sufficient duration then when activity resumes the network has no

392 memory of the location of the previous bump. The spatial representation

393 necessary for path integration is then lost. This loss of bump stability can be

394 prevented by synaptic or intrinsic conductances with slow dynamics

395 (Navratilova et al., 2012; Pastoll et al., 2013; Solanka et al., 2015). For

396 example, on the start of each new theta cycle the residual excitatory NMDA

397 receptor current ensures bumps re-form in their previous location (Figure 4).

12

398   While there is evidence that NMDA receptors in entorhinal interneurons have
399   sufficiently slow kinetics to perform this role (Jones and Buhl, 1993), it is
400   possible that other biophysical processes that have slow dynamics such as
401   intracellular Ca^{2+} signalling or kinetics of the action potential
402   afterhyperpolarisation could also stabilise attractor states across theta cycles
403   (Navratilova et al., 2012). Alternatively, theta modulation may not completely
404   inactivate entorhinal networks, in which case bump location could be
405   maintained through neurons that remain active across the full theta cycle.
406   Further experimental testing of these ideas will require a better understanding
407   of cellular mechanisms underlying modulation of entorhinal activity during
408   theta states.
409
410   **Noise enables independent control of theta nested gamma oscillations**
411   **and grid firing by modulation of excitatory-inhibitory interactions**
412   Because E-I models account for rate coded grid computation and gamma
413   frequency network activity, they provide an opportunity to investigate
414   relationships between these phenomena. Many cognitive functions, in addition
415   to spatial computation by grid networks, are associated with modulation of
416   gamma activity (Uhlhaas and Singer, 2012). In turn, both cognitive function
417   and gamma activity correlate with changes in E-I interactions. However, the
418   causal relationships between the strength of excitatory and inhibitory
419   synapses, gamma oscillations and computations that might underlie key
420   cognitive functions have been difficult to establish. Systematic investigation of
421   E-I models suggests that these relationships are complex (Solanka et al.
422   2015). First, nested gamma oscillations and grid firing are both promoted by
423   an optimal level of noise within a network. If noise is too low seizure-like
424   states that suppress grid firing tend to emerge, whereas if noise is too high
425   grid fields drift and gamma becomes less coherent. Second, intermediate
426   noise levels maximise the range of excitatory and inhibitory synaptic strengths
427   that support grid firing. Third, gamma activity is a poor predictor of grid firing.
428   Thus, varying the strength of inhibitory or excitatory connections can tune the
429   frequency and power of gamma oscillations without affecting grid firing.
430   Fourth, tuning of intrinsic connections could be used to modulate oscillation-
431   based codes while maintaining grid firing, for example to determine the

13

432 response of downstream neurons to convergent input from different grid
433 modules. Thus, synchronisation of gamma activity between grid modules
434 might promote, and discordant tuning of gamma between modules might
435 oppose, downstream integration. Therefore, the potential for independent
436 control of gamma oscillations and grid firing, even though both phenomena
437 arise from a common circuit mechanism, has implications for physiological
438 and pathological states of MEC circuits.
439
440

441 **Conclusion**
442 Because multiple abstract models are able to produce grid-like periodic spatial
443 firing patterns, additional experimental constraints are required to establish
444 mechanisms used by the brain to generate grid firing. We have considered
445 evidence that continuous attractor networks that use velocity inputs to
446 compute grid codes for location can be implemented through E-I interactions
447 that are consistent with known properties of microcircuits in the MEC. When
448 implemented with realistic neuronal dynamics these models also account for
449 theta nested gamma oscillations, although so far they are unable to explain
450 theta phase precession in two dimensions without incorporation of additional
451 mechanisms for path integration. Critical future tests of continuous attractor
452 network hypotheses for grid firing include evaluation of predictions for the
453 firing patterns and connectivity of excitatory and inhibitory cell populations. E-I
454 models make further assumptions concerning integration of velocity signals
455 (Pastoll et al. 2013), error correction by place and border input (Guanella et
456 al., 2007; Hardcastle et al., 2015; Pastoll et al., 2013; Sreenivasan and Fiete,
457 2011) and sources of tonic drive (Bonnevie et al., 2013; Burak and Fiete,
458 2009; Pastoll et al., 2013) that we have not considered here. Experimental
459 evidence for how these signals are integrated by MEC circuits will further
460 constrain possible models. Progress in establishing experimentally
461 constrained models for spatial representation by cell populations in the MEC
462 may serve as a proof of principle for understanding cellular and synaptic
463 mechanisms for high-level computations by cortical circuits in general.
464
465

14

466

References

468 Barry, C., Hayman, R., Burgess, N., and Jeffery, K.J. (2007). Experience-dependent
469 rescaling of entorhinal grids. Nat Neurosci *10*, 682-684.
470 Bonnevie, T., Dunn, B., Fyhn, M., Hafting, T., Derdikman, D., Kubie, J.L., Roudi, Y.,
471 Moser, E.I., and Moser, M.B. (2013). Grid cells require excitatory drive from the
472 hippocampus. Nat Neurosci *16*, 309-317.
473 Brody, C.D., Romo, R., and Kepecs, A. (2003). Basic mechanisms for graded
474 persistent activity: discrete attractors, continuous attractors, and dynamic
475 representations. Curr Opin Neurobiol *13*, 204-211.
476 Burak, Y., and Fiete, I.R. (2009). Accurate path integration in continuous attractor
477 network models of grid cells. PLoS Comput Biol *5*, e1000291.
478 Burgess, N., Barry, C., and O'Keefe, J. (2007). An oscillatory interference model of
479 grid cell firing. Hippocampus *17*, 801-812.
480 Burgess, N., and O'Keefe, J. (2011). Models of place and grid cell firing and theta
481 rhythmicity. Curr Opin Neurobiol.
482 Bush, D., and Burgess, N. (2014). A hybrid oscillatory interference/continuous
483 attractor network model of grid cell firing. J Neurosci *34*, 5065-5079.
484 Chrobak, J.J., and Buzsaki, G. (1998). Gamma oscillations in the entorhinal cortex
485 of the freely behaving rat. J Neurosci *18*, 388-398.
486 Colgin, L.L., Denninger, T., Fyhn, M., Hafting, T., Bonnevie, T., Jensen, O., Moser,
487 M.B., and Moser, E.I. (2009). Frequency of gamma oscillations routes flow of
488 information in the hippocampus. Nature *462*, 353-357.
489 Conklin, J., and Eliasmith, C. (2005). A controlled attractor network model of path
490 integration in the rat. J Comput Neurosci *18*, 183-203.
491 Couey, J.J., Witoelar, A., Zhang, S.J., Zheng, K., Ye, J., Dunn, B., Czajkowski, R.,
492 Moser, M.B., Moser, E.I., Roudi, Y.*, et al.* (2013). Recurrent inhibitory circuitry as a
493 mechanism for grid formation. Nat Neurosci *16*, 318-324.
494 Dhillon, A., and Jones, R.S. (2000). Laminar differences in recurrent excitatory
495 transmission in the rat entorhinal cortex in vitro. Neuroscience *99*, 413-422.
496 Domnisoru, C., Kinkhabwala, A.A., and Tank, D.W. (2013). Membrane potential
497 dynamics of grid cells. Nature *495*, 199-204.
498 Eliasmith, C. (2005). A unified approach to building and controlling spiking
499 attractor networks. Neural Comput *17*, 1276-1314.
500 Fiete, I.R., Burak, Y., and Brookings, T. (2008). What grid cells convey about rat
501 location. J Neurosci *28*, 6858-6871.
502 Fourcaud-Trocme, N., Hansel, D., van Vreeswijk, C., and Brunel, N. (2003). How
503 spike generation mechanisms determine the neuronal response to fluctuating
504 inputs. J Neurosci *23*, 11628-11640.
505 Fuhs, M.C., and Touretzky, D.S. (2006). A spin glass model of path integration in
506 rat medial entorhinal cortex. J Neurosci *26*, 4266-4276.
507 Giocomo, L.M., Moser, M.B., and Moser, E.I. (2011). Computational models of grid
508 cells. Neuron *71*, 589-603.
509 Gonzalez-Sulser, A., Parthier, D., Candela, A., McClure, C., Pastoll, H., Garden, D.,
510 Surmeli, G., and Nolan, M.F. (2014). GABAergic projections from the medial
511 septum selectively inhibit interneurons in the medial entorhinal cortex. J
512 Neurosci *34*, 16739-16743.

513 Guanella, A., Kiper, D., and Verschure, P. (2007). A model of grid cells based on a
514 twisted torus topology. Int J Neural Syst *17*, 231-240.
515 Hafting, T., Fyhn, M., Bonnevie, T., Moser, M.B., and Moser, E.I. (2008).
516 Hippocampus-independent phase precession in entorhinal grid cells. Nature *453*,
517 1248-1252.
518 Hafting, T., Fyhn, M., Molden, S., Moser, M.B., and Moser, E.I. (2005).
519 Microstructure of a spatial map in the entorhinal cortex. Nature *436*, 801-806.
520 Hardcastle, K., Ganguli, S., and Giocomo, L.M. (2015). Environmental boundaries
521 as an error correction mechanism for grid cells. Neuron *86*, 827-839.
522 Hasselmo, M.E., Giocomo, L.M., and Zilli, E.A. (2007). Grid cell firing may arise
523 from interference of theta frequency membrane potential oscillations in single
524 neurons. Hippocampus *17*, 1252-1271.
525 Heys, J.G., Rangarajan, K.V., and Dombeck, D.A. (2014). The functional micro-
526 organization of grid cells revealed by cellular-resolution imaging. Neuron *84*,
527 1079-1090.
528 Jones, R.S., and Buhl, E.H. (1993). Basket-like interneurones in layer II of the
529 entorhinal cortex exhibit a powerful NMDA-mediated synaptic excitation.
530 Neurosci Lett *149*, 35-39.
531 Kitamura, T., Pignatelli, M., Suh, J., Kohara, K., Yoshiki, A., Abe, K., and Tonegawa,
532 S. (2014). Island cells control temporal association memory. Science *343*, 896-
533 901.
534 Klink, R., and Alonso, A. (1997). Morphological characteristics of layer II
535 projection neurons in the rat medial entorhinal cortex. Hippocampus *7*, 571-583.
536 Kropff, E., Carmichael, J.E., Moser, M.B., and Moser, E.I. (2015). Speed cells in the
537 medial entorhinal cortex. Nature *523*, 419-424.
538 Mathis, A., Herz, A.V., and Stemmler, M. (2012). Optimal population codes for
539 space: grid cells outperform place cells. Neural Comput *24*, 2280-2317.
540 McNaughton, B.L., Barnes, C.A., Gerrard, J.L., Gothard, K., Jung, M.W., Knierim, J.J.,
541 Kudrimoti, H., Qin, Y., Skaggs, W.E., Suster, M., *et al.* (1996). Deciphering the
542 hippocampal polyglot: the hippocampus as a path integration system. J Exp Biol
543 *199*, 173-185.
544 McNaughton, B.L., Battaglia, F.P., Jensen, O., Moser, E.I., and Moser, M.B. (2006).
545 Path integration and the neural basis of the 'cognitive map'. Nat Rev Neurosci *7*,
546 663-678.
547 Navratilova, Z., Giocomo, L.M., Fellous, J.M., Hasselmo, M.E., and McNaughton, B.L.
548 (2012). Phase precession and variable spatial scaling in a periodic attractor map
549 model of medial entorhinal grid cells with realistic after-spike dynamics.
550 Hippocampus *22*, 772-789.
551 Pastoll, H., Ramsden, H.L., and Nolan, M.F. (2012). Intrinsic electrophysiological
552 properties of entorhinal cortex stellate cells and their contribution to grid cell
553 firing fields. Front Neural Circuits *6*, 17.
554 Pastoll, H., Solanka, L., van Rossum, M.C., and Nolan, M.F. (2013). Feedback
555 inhibition enables theta-nested gamma oscillations and grid firing fields. Neuron
556 *77*, 141-154.
557 Ray, S., Naumann, R., Burgalossi, A., Tang, Q., Schmidt, H., and Brecht, M. (2014).
558 Grid-layout and theta-modulation of layer 2 pyramidal neurons in medial
559 entorhinal cortex. Science *343*, 891-896.
560 Reifenstein, E.T., Kempter, R., Schreiber, S., Stemmler, M.B., and Herz, A.V. (2012).
561 Grid cells in rat entorhinal cortex encode physical space with independent firing

562 fields and phase precession at the single-trial level. Proc Natl Acad Sci U S A *109*,
563 6301-6306.
564 Remme, M.W., Lengyel, M., and Gutkin, B.S. (2010). Democracy-independence
565 trade-off in oscillating dendrites and its implications for grid cells. Neuron *66*,
566 429-437.
567 Samsonovich, A., and McNaughton, B.L. (1997). Path integration and cognitive
568 mapping in a continuous attractor neural network model. J Neurosci *17*, 5900-
569 5920.
570 Sargolini, F., Fyhn, M., Hafting, T., McNaughton, B.L., Witter, M.P., Moser, M.B., and
571 Moser, E.I. (2006). Conjunctive representation of position, direction, and velocity
572 in entorhinal cortex. Science *312*, 758-762.
573 Schmidt-Hieber, C., and Hausser, M. (2013). Cellular mechanisms of spatial
574 navigation in the medial entorhinal cortex. Nat Neurosci *16*, 325-331.
575 Seung, H.S., Lee, D.D., Reis, B.Y., and Tank, D.W. (2000). Stability of the memory of
576 eye position in a recurrent network of conductance-based model neurons.
577 Neuron *26*, 259-271.
578 Solanka, L., van Rossum, M.C., and Nolan, M.F. (2015). Noise promotes
579 independent control of gamma oscillations and grid firing within recurrent
580 attractor networks. Elife *4*, e06444.
581 Sreenivasan, S., and Fiete, I. (2011). Grid cells generate an analog error-
582 correcting code for singularly precise neural computation. Nat Neurosci *14*,
583 1330-1337.
584 Stensola, H., Stensola, T., Solstad, T., Froland, K., Moser, M.B., and Moser, E.I.
585 (2012). The entorhinal grid map is discretized. Nature *492*, 72-78.
586 Sun, C., Kitamura, T., Yamamoto, J., Martin, J., Pignatelli, M., Kitch, L.J., Schnitzer,
587 M.J., and Tonegawa, S. (2015). Distinct speed dependence of entorhinal island
588 and ocean cells, including respective grid cells. Proc Natl Acad Sci U S A *112*,
589 9466-9471.
590 Tang, Q., Burgalossi, A., Ebbesen, C.L., Ray, S., Naumann, R., Schmidt, H., Spicher,
591 D., and Brecht, M. (2014). Pyramidal and stellate cell specificity of grid and
592 border representations in layer 2 of medial entorhinal cortex. Neuron *84*, 1191-
593 1197.
594 Tiesinga, P., and Sejnowski, T.J. (2009). Cortical enlightenment: are attentional
595 gamma oscillations driven by ING or PING? Neuron *63*, 727-732.
596 Uhlhaas, P.J., and Singer, W. (2012). Neuronal dynamics and neuropsychiatric
597 disorders: toward a translational paradigm for dysfunctional large-scale
598 networks. Neuron *75*, 963-980.
599 Varga, C., Lee, S.Y., and Soltesz, I. (2010). Target-selective GABAergic control of
600 entorhinal cortex output. Nat Neurosci *13*, 822-824.
601 Widloski, J., and Fiete, I.R. (2014). A Model of Grid Cell Development through
602 Spatial Exploration and Spike Time-Dependent Plasticity. Neuron *83*, 481-495.
603 Widloski, J., and Fiete, I.R. (2015). Cortical microcircuit determination through
604 perturbation and sparse sampling in grid cells. bioRxiv
605 http://dx.doi.org/10.1101/019224.
606 Yoon, K., Buice, M.A., Barry, C., Hayman, R., Burgess, N., and Fiete, I.R. (2013).
607 Specific evidence of low-dimensional continuous attractor dynamics in grid cells.
608 Nat Neurosci *16*, 1077-1084.
609 Zhang, K. (1996). Representation of spatial orientation by the intrinsic dynamics
610 of the head-direction cell ensemble: a theory. J Neurosci *16*, 2112-2126.

611 Zilli, E.A. (2012). Models of grid cell spatial firing published 2005-2011. Front
612 Neural Circuits *6*, 16.
613
614
615 **Additional information**

616

617 Competing interests

618 None of the authors has any conflicts of interest.

619

627

628 **Figure 1. Components of a generic E-I model for generation of grid firing**
629 **and nested gamma oscillations**
630 Integration of velocity input by continuous attractor networks built from
631 interacting excitatory and inhibitory neurons can generate grid firing fields.
632 When the networks receive a theta modulated input they generate gamma
633 frequency output that is modulated at theta frequency. A spatial input is
634 required to oppose drift in the grid representation. Data are from Pastoll et al.
635 (2013).
636
637

638 **Figure 2. Single and multi-bump attractor model of grid firing have**
639 **distinct circuit organisation**
640 In single bump models grid firing of excitatory cells can be generated by
641 synaptic profiles that produce either surround excitation or surround inhibition.
642 The surround connectivity is strongest for connections to neurons at a
643 distance of about one half the width of the sheet. Each neuron makes
644 divergent connections to many target neurons, and receives convergent input
645 from many pre-synaptic neurons. In multi-bump networks the strongest
646 connections are onto neurons at a much shorter distance relative to the size
647 of the sheet. The upper graphs plot synaptic strength as a function of position
648 in the neural sheet, which is given a width of one. The plots below schematise
649 the resulting E-I connectivity, illustrate the organisation of activity in the neural
650 sheet and the organisation of excitatory cell activity in three dimensions. The
651 connectivity profiles shown for the multi-bump models are based on networks
652 containing only inhibitory neurons, with either surround inhibition (Burak and
653 Fiete, 2009) or local inhibition (Couey et al., 2013). The networks could be
654 considered as having dedicated interneurons receiving input from each
655 excitatory neuron.
656
657

658 **Figure 3. Spatial firing of interneurons in E-I attractor models**
659 (A) Schematic organisation of an E-I network with additional random place
660 field inputs to each interneuron (left). Example firing fields of I cells (middle)
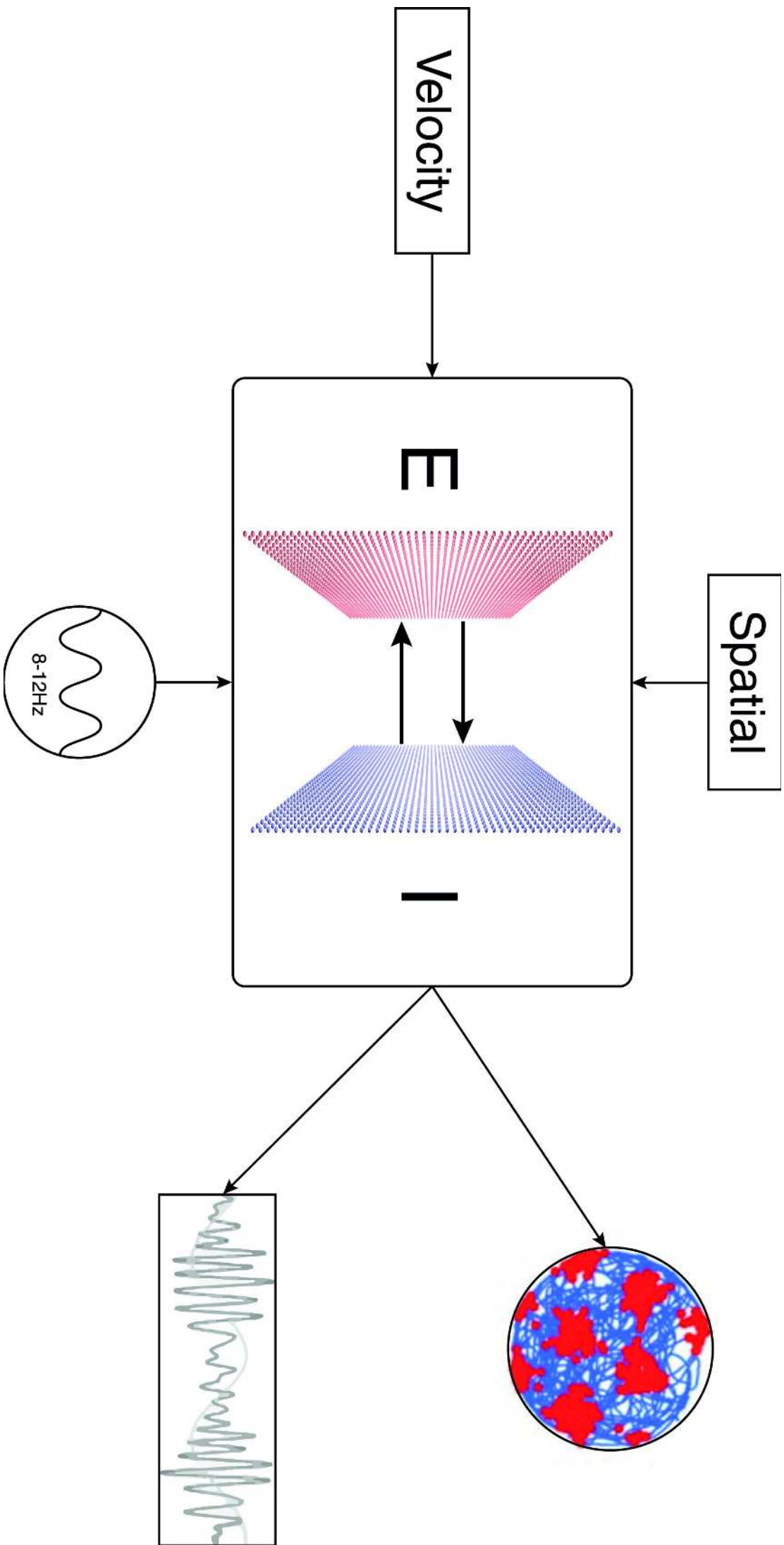661 and E cells (right) are shown adjacent to the schematised neurons. (B)

662   Histograms of the spatial sparsity (upper) and gridness score (lower) for E-I

663   networks simulated as in (A). Note that most interneurons and many

664   excitatory cells have grid scores < 0.5. Data are from Solanka et al. 2015
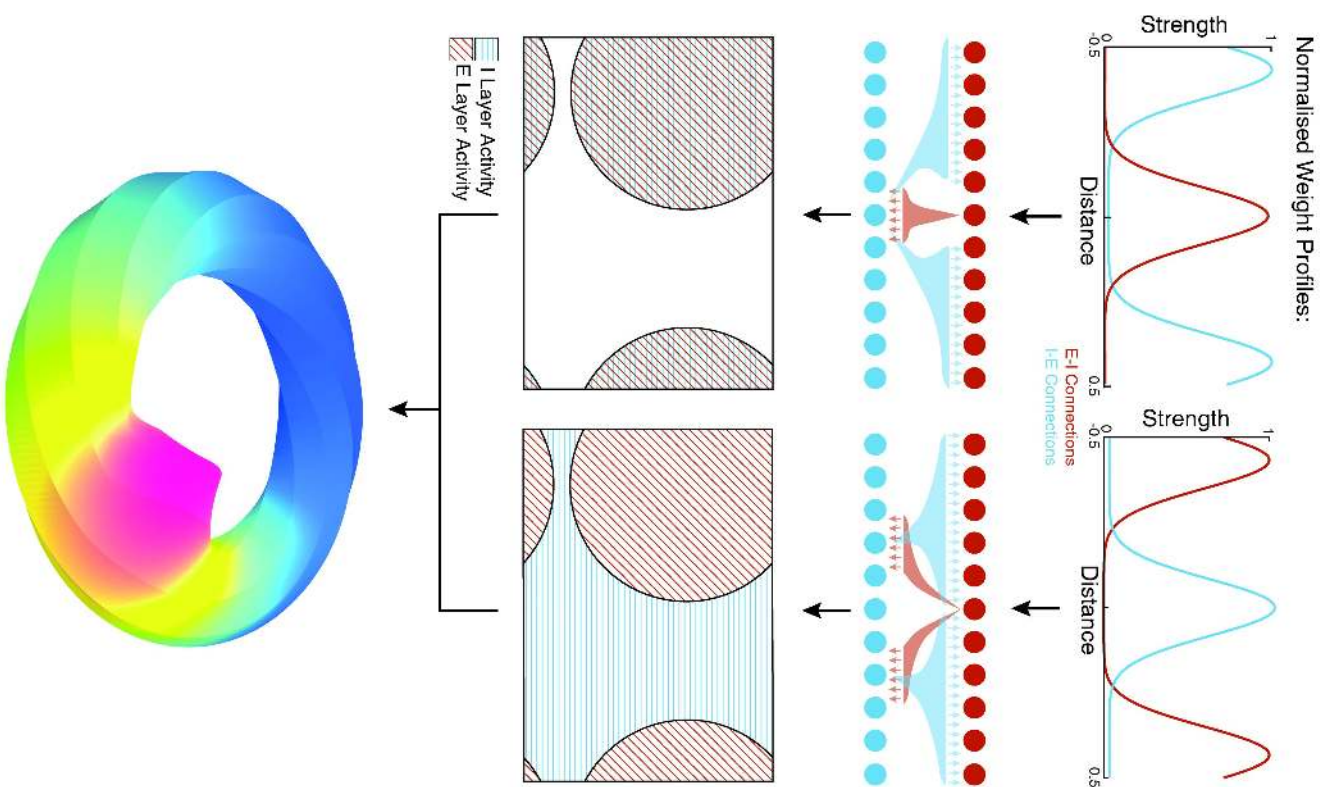
665

666

667   **Figure 4. Theta nested gamma activity in E-I models**

668   Spike rasters for E cells (red) and I cells (blue) during two theta cycles (grey).

669   The excitatory synaptic input to a representative I cell is illustrated below.

670   Note that a substantial residual inward current (blue shading) is maintained

671   during the phase of the theta oscillation when spike activity of excitatory cells

672   is reduced. The residual current enables the bump of activity to be maintained

673   across theta cycles. Data are from Pastoll et al. (2013) and Solanka et al.
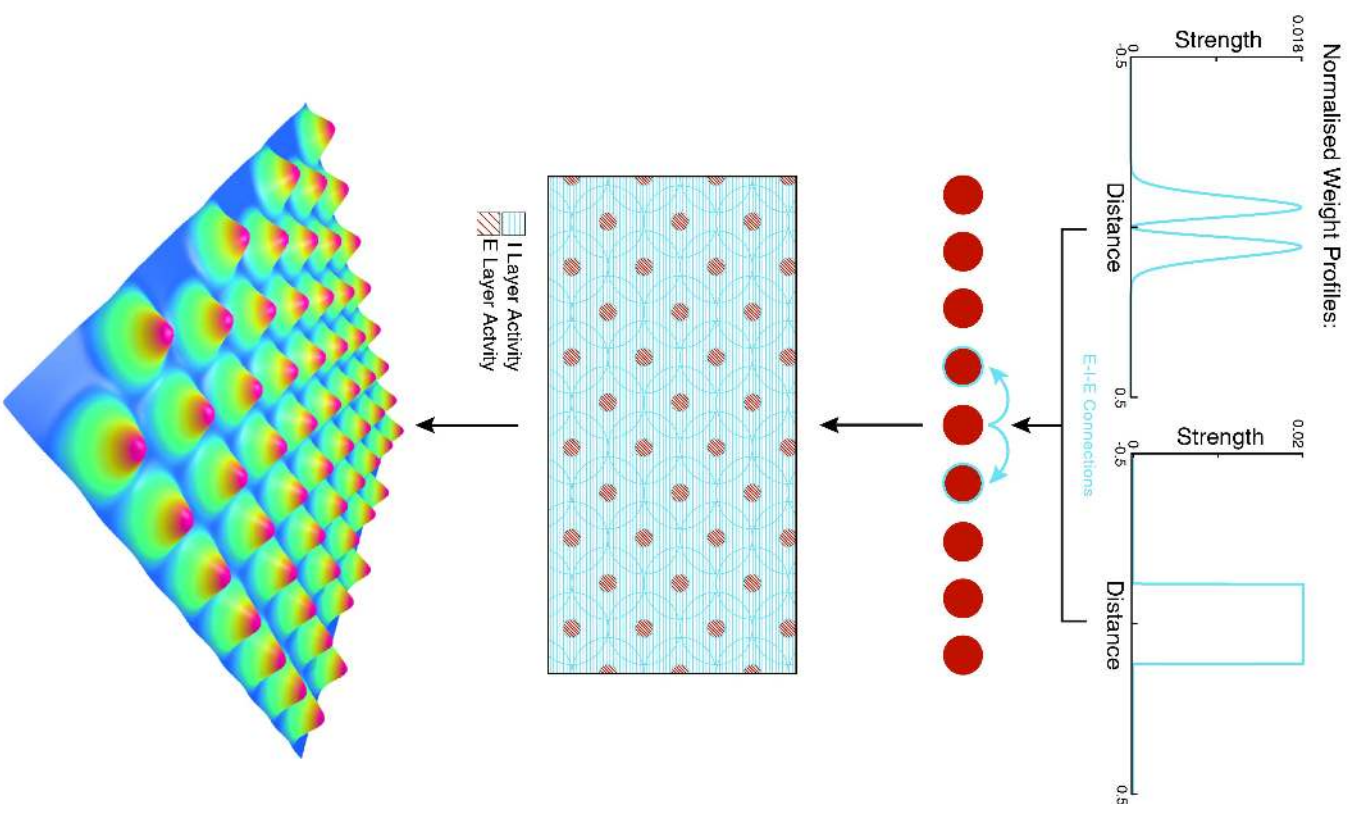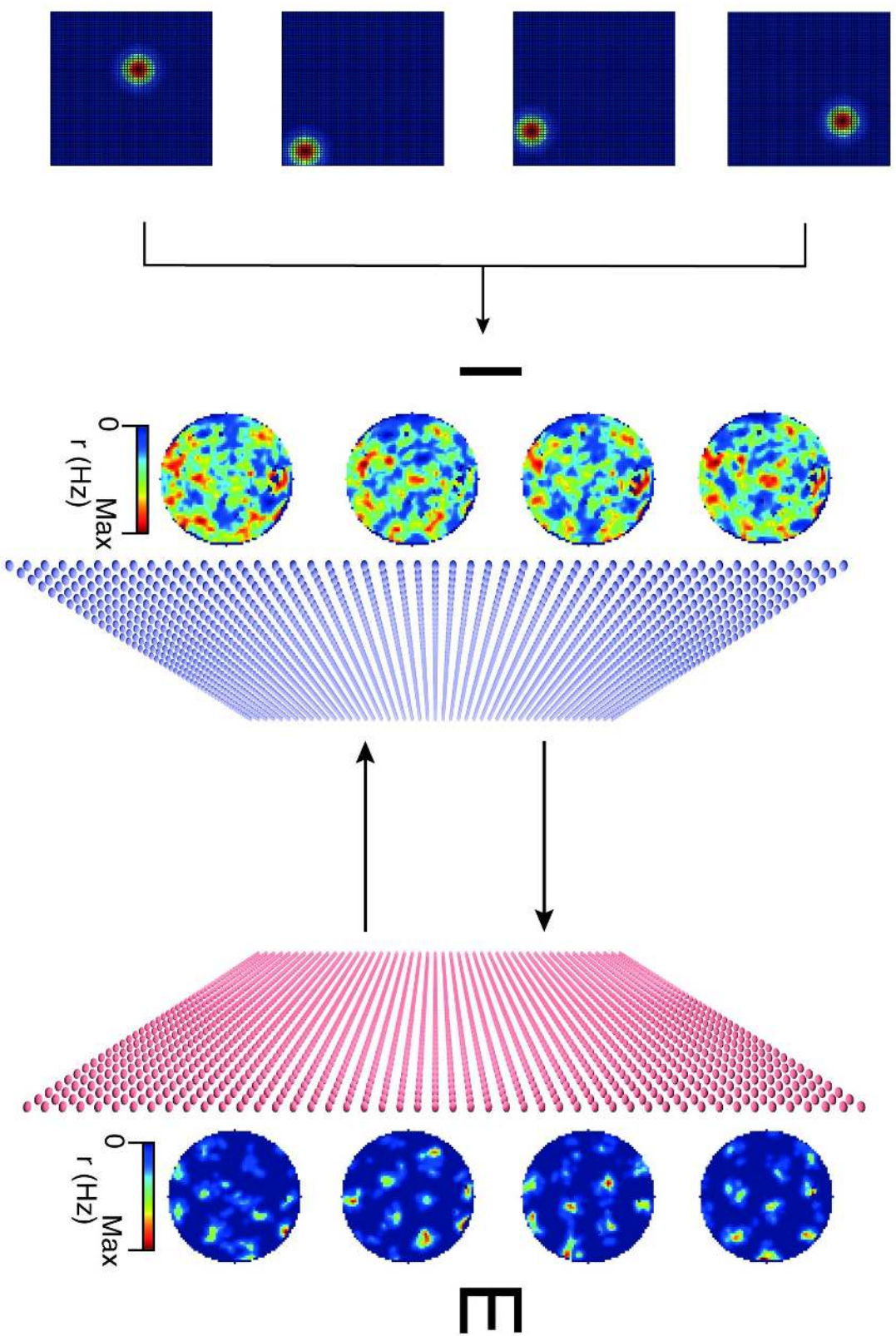
674   (2015).

Velocity

E

8-12Hz

Spatial

I

A Single Bump

Normalised Weight Profiles:

E-I Connections
I-E Connections

I Layer Activity
E Layer Activity

B Multi-Bump

Normalised Weight Profiles:

E-I-E Connections

I Layer Activity
E Layer Activity

A

I

r (Hz) 0 — Max

E

r (Hz) 0 — Max

B

Count

150

100

50

0

−0.5   0.0   0.5   1.0   1.5

Gridness score

Count

1000

750

500

250

0

0.0   0.2   0.4   0.6   0.8   1.0

Spatial sparsity

E cells

I cells
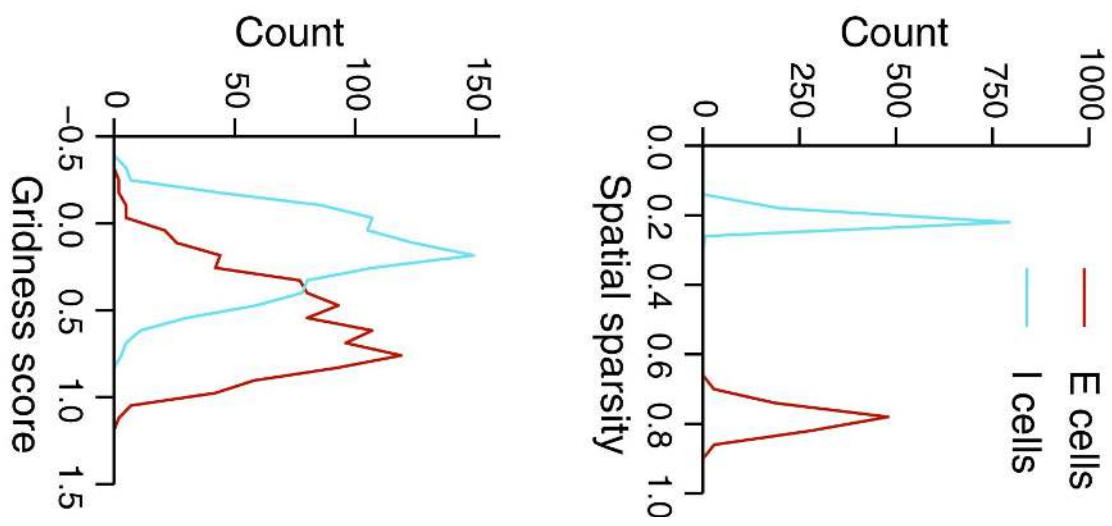
Theta
Envelope

Excitatory Cell
Spikes

Inhibitory Cell
Spikes

0

-200

Interneuron
Membrane
Current

-400

-600